Unbiased stereological estimation of the total number of synapses in a brain region

Geinisman, Y.; Gundersen, H.J.G.; Zee, E. van der

Published in:
Journal of Neurocytology

DOI:
10.1007/BF02284843

Publication date:
1996

Journal of Neurocytology **25**, 805–819 (1996)

Unbiased stereological estimation of the total number of synapses in a brain region

Y. GEINISMAN[1]*, H. J. G. GUNDERSEN[2], E. VAN DER ZEE[1] and M. J. WEST[3]

[1]*Department of Cell and Molecular Biology, Northwestern University Medical School, 303 East Chicago Avenue, Chicago, Illinois 60611, USA*

[2]*Stereological Research Laboratory and* [3]*Institute for Neurobiology, University of Aarhus, 8000 Aarhus, Denmark*

25th Anniversary Issue

Summary

Modern stereological methods have been used to make unbiased estimates of the total number of synapses in the striatum radiatum of the hippocampal CA1 region of five rabbits. The approach used involved a two stage analysis and is generally applicable to all parts of the nervous system. During the first stage of the analysis, the reference volume was estimated by point counting, at the light microscope level, according to the Cavalieri principle. During the second stage, the numerical density of synapses was estimated with disectors at the electron microscopic level. The total number of synapses was calculated as the product of the numerical density and the volume of the region. The sampling with points and disectors was carried out in all three dimensions of the entire CA1 region in a manner that ensured that all parts of the region and all synapses within it had equal probabilities of being sampled. An analysis of the precision of the estimate of total synapse number has been performed in terms of the variances of volume and synaptic numerical density at different levels of sampling, i.e. at the level of points, sections, individual animals and group of animals. Detailed descriptions of the procedures used to estimate the total number of synapses, evaluate the precision of the estimates, and optimize the sampling scheme are provided.

Introduction

The total number of synapses in a region or subregion of the nervous system is a parameter of primary significance when evaluating the functional capacity of a neural structure. Synapses represent the points of communication between neurons and, in spite of the unresolved issues about the differential roles and efficacy of synapses of different types and at different positions on postsynaptic elements, their number is a fundamental expression of the amount of neural input to the neurons of a region. Together with information about the number of neurons, they provide a structural framework in which to interpret changes in the functional capacity of neural structures. The quantitation of subtypes of synapses can eventually yield additional information about the dynamics of neural structures and organization of their components. Until recently, appropriate methods for obtaining reliable measures of the number of synapses have not been available. As a consequence, the literature dealing with changes in synapse number is rife with seemingly contradictory data (e.g., see Geinisman *et al.*, 1995).

A new generation of stereological principles have been developed in recent years (Sterio, 1984; Brændgaard & Gundersen, 1986; Gundersen, 1986; Gundersen *et al.*, 1988; Pakkenberg & Gundersen, 1988; West, 1993; Mayhew & Gundersen, 1996) that have the potential for forming the basis of a reliable method for estimating synapse number. The application of these principles has resulted in the development of sampling and counting techniques that can be used to make unbiased estimates of the total number of objects in a defined region of biological tissue. The salient features of the methods for obtaining these estimates are that (1) all parts of the region under consideration have an equal probability of being sampled and (2) objects are directly counted in a known volume of tissue without having to make any assumptions about the size, shape, or orientation of the objects. When these techniques are properly applied, the resulting estimates are unbiased in the sense that the mean of repeated estimates will approach the true number without limit. That is, they will not systematically deviate from the true value as they might when the selective sampling and assumption based counting rules of previously available techniques are used.

*To whom correspondence should be addressed.

0300–4864/96

Although these same principles form the basis of the recently described methods for estimating the number of neurons in light microscopic preparations (Pakkenberg & Gundersen, 1988; Brændgaard *et al.*, 1990; West & Gundersen, 1990; West *et al.*, 1991; West, 1993), the necessity for the use of EM images when quantifying synapses introduces a number of practical constraints on the approaches available. For example, there are two basic approaches for obtaining unbiased estimates of neuron number. One involves a two-step sampling scheme like that used here. Accordingly, the volume of the region of interest, i.e. the reference volume, $V(ref)$, is first estimated from a relatively small number of sections selected in a systematic random manner along the entire extent of the region. Second, the numerical density of neurons, N_V, is estimated from a series of disectors placed uniformly within the same sections. The product of the two estimates gives $N(neur)$, the number of neurons, $N(neur) = V(ref) \cdot N_V$.

The other approach, the fractionator (Gundersen, 1986), involves determining the number of neurons (again with disectors) in a known fraction of the volume of the region of interest. The first step in fractionator sampling usually involves the sampling of a known fraction of the sections that are generated by exhaustive sectioning. In the case of regions that result in large and unwieldy numbers of sections, additional levels of block subsampling can be introduced. Because it is important with fractionator sampling to keep track of all of the sections cut (be they either from the entire region or a known fraction of the blocks from larger regions), in order to determine what fraction of the region is being quantified, this approach can be very demanding when working at the EM level. To avoid the extensive subsampling and exhaustive ultramicrotomy inherent in the application of fractionator sampling to EM material, we have here adopted the $V(ref) \cdot N_V$ approach to synapse quantitation.

There has been one previous description of a method for obtaining unbiased estimates of total synapse number based on the principles outlined above This technique, referred to as the 'double disector' (Gundersen *et al.*, 1988) involves the use of the same set of serial ultrathin sections to count synapses and neurons. The disectors used to count synapses were adjacent sections and those used to count neurons were separated by a relatively large, but known, number of sections. The relative densities of the synapses and neurons could then be used to determine the ratio of synapses to postsynaptic neurons. An unbiased estimate of the total number of neurons was then obtained from light microscopic material and multiplied by the ratio of synapses per neuron to obtain an estimate of the total synapse number. The advantage of the double disector is that it does not require knowledge of the thickness of the ultrathin sections used in the analysis. This method is limited, however, by the extensive ultramicrotomy required to obtain an adequate sample of neurons at the EM level and has not yet been used to make rigorous estimates of total synapse number as done in this study.

Because the methodology employed is designed to obtain *estimates* of total number, not determinations, these estimates have a certain precision or variance, which is related to the amount of sampling performed. Specific procedures have been developed in recent years to evaluate the precision of the resulting estimates and to assess the optimal number of animals or individuals, sections, and synapses that need to be analyzed in a specific study (Gundersen & Jensen, 1987). Detailed examples of how data obtained with the methodology described here can be analysed with these procedures are also presented.

Materials and methods

In order to obtain unbiased estimates of the total number of synapses, it is necessary to ensure that the sampling performed during both phases of the $V(ref) \cdot N_V$ analysis is unbiased. In the case of the $V(ref)$ determinations, we used a systematic random selection of histological sections for point counting. Disectors consisting of ultrathin sections were used to count synapses and thereby make estimates of N_V. The disector (Sterio, 1984) is a three-dimensional stereological probe which, in its simplest form, is composed of two adjacent sections. It has the unique feature of sampling objects in direct proportion to their number and thereby provides a tool for number weighted counts of objects. The volume of a disector is determined by the area of the sections and the distance between them. An object is considered to be in a disector if a unique prespecified point of the object lies in the disector. For objects of finite volume (like synapses, neurons, etc.) one usually specifies the leading edge of the particle on the axis of sectioning, i.e. the first recognizable profile of the structure. Accordingly, an object is considered to be in the disector if it can be identified in the second section of the disector, but not the first. One has only to ensure that the distance between the two sections is less that the shortest dimension of the objects of interest so that none escape detection. In the case of sections that are large relative to the structures being counted, subsampling of the regions of interest can be performed with unbiased areal counting frames (Gundersen, 1977). Because disectors sample objects in proportion to their number, the resulting counts are not influenced by the size, shape, and orientation of the objects. As a consequence, the counts are not subject to the potential biases introduced by assumptions about these features required with previously available techniques that were based on the use of single two dimensional probes (i.e., sections). In addition, provided the objects of interest can be potentially identified on at least one section (the only requirement for the application of disector counting), the counts will be unaffected by truncation and overprojection (Coggeshall & Lekan, 1996; Saper, 1966).

Perfusion-fixation

Five New Zealand albino female rabbits of 8–10 weeks of age

(*Oryctolagus cuniculus*) were used in this study. Animals were deeply anaesthetized with a combination of Xylazine (6 mg kg^{-1}, i.m.) and Ketamine hydrochloride (45 mg kg^{-1}, i.m.) followed 15 min later by Pentobarbital sodium (75 mg kg^{-1}, i.m.). Transcardiac perfusion was then performed in three consecutive steps: (1) phosphate buffered saline containing Heparin sodium (10 units ml^{-1}) injected at a rate of 50 ml min^{-1} for 45 s (~40 ml); (2) 1% paraformaldehyde, 1.25% glutaraldehyde and 0.02 mM $CaCl_2$ in 0.12 M phosphate buffer (pH 7.3) perfused initially at a rate of 50 ml min^{-1} for 10 min (500 ml) and thereafter at a rate of 25 ml min^{-1} for additional 20 min (500 ml); (3) the same fixative at twice the aldehyde concentration delivered at a rate of 25 ml min^{-1} for 12 min (300 ml). All solutions were warmed to 37° C and administered with a Masterflex peristaltic pump (Cole-Parmer Instrument Co., Niles, Illinois). After the perfusion, animals were placed in sealed plastic bags and kept in a refrigerator for 2 h at 4° C. The brain was then removed, the left hemisphere put in a vial mounted on a tissue rotator and postfixed in the double strength fixative at 4° C overnight.

Preparing a systematic random series of histological sections through the CA1 region

The left hippocampal formation was dissected free and cut into a number of 1.5 mm thick slabs with the aid of a tissue chopper (Stoelting Co., Niles, Illinois) equipped with a microdrive. The slab thickness was chosen so that 10–15 histological sections, spaced at equal intervals along the entire septo-temporal axis, would be obtained from the corresponding faces of the slabs. It was determined *a priori*, on the basis of other studies (West & Gundersen, 1990; West, 1993), that the analysis of this number of sections would result in a precision compatible with the goals of this study (i.e., the mean coefficient of error, *CE*, of the estimates obtained from individual animals should be under 10%, see below).

Because the delineation of the CA1 region is more readily carried out on sections that approximate the transverse plane of the septo-temporal axis of the hippocampus and because the sections used in the analysis must be parallel to each other, the natural 'U'-shaped curvature of the septo-temporal axis (Fig. 1a) was straightened prior to the cutting of the slabs (Gaarskjaer, 1978). To accomplish this, the surface of the hippocampal formation, which is opposite to that overlying the CA1 region, was dried with a filter paper and attached at the septal end to the tissue chopper stage with a rapidly drying glue. The hippocampal formation was then manually straightened along the septo-temporal axis and the remaining surface glued to the stage. Following this procedure, the rabbit hippocampal formation had a length of 18–21 mm and could be divided into 12–14, 1.5 mm thick slabs. During the preparation of the slabs, the tissue was bathed in cold (4° C) 0.12 M phosphate buffer. Using a razor blade mounted on the tissue chopper, the hippocampal formation was cut in the plane perpendicular to an imaginary straight line connecting the septal and temporal poles (Fig. 1b). The position of the first cut within the first 1.5 mm interval from the septal pole was determined randomly by choosing a random number from 1 to 150 and moving the chopper microdrive to a corresponding setting. The subsequent cuts were placed at a uniform interval of 1.5 mm from each other.

Each tissue slab was transferred into a Wheaton specimen vial mounted on a tissue rotator. Slabs were rinsed in cold 0.12 M phosphate buffer (three changes, 5 min each), treated with OsO_4 (2% solution in 0.12 M phosphate buffer for 90 min at 4° C) and rinsed again in the buffer (three changes, 5 min each at room temperature). Subsequently, the slabs were dehydrated in ethanol solutions of increasing concentrations (50, 70 and 90%–5 min each; 95%–5 min three times; and 100%–15 min two times), treated with propylene oxide (two changes, 15 min each), left overnight in a mixture (1 : 1) of propylene oxide-Araldite 502, flat embedded in Araldite using disk block embedding molds, and cured in an oven at 60° C for 48 h.

Estimation of the average thickness of fixed and embedded tissue slabs

A set of systematic random histological sections through the CA1 region was obtained by cutting semithin (3 μm thick) sections from the septal face of each tissue slab. The distance between the sections was equal to the thickness of the embedded slabs. (It is important to note that the estimation of both the reference volume, $V(ref)$, and the synaptic numerical density, N_V, was carried out on the plastic embedded material). Since it could not be assumed that the thickness of the slabs was unaltered during the embedding procedure, the average slab thickness, $\bar{T}$, was determined and used as an estimate of a uniform interval between histological sections. For this purpose, each block of Araldite containing a tissue slab was covered with a thin layer of microscope immersion oil of a low viscosity to obtain a sharp microscopic image of the osmicated tissue embedded in the plastic. The slab thickness was then measured using a Zeiss inverted microscope equipped with an eye-piece micrometer at a total magnification of 18 ×.

Delineation of the synapse-containing layer

Each semithin section was placed on a drop of distilled water on an ethanol-cleaned microscope slide, dried overnight on a slide-warming plate at 60° C, stained with Azur II-Methylene Blue (Richardson *et al.*, 1960), rinsed with distilled water, and dried again. In such Nissl-stained sections, the CA1 region of the rabbit hippocampus can be reliably identified. Although the CA1 region is continuous with the CA2 field and subicular complex, it can be unequivocally distinguished from these two hippocampal subdivisions. Giant pyramidal cells, which are typical of CA3 and which are also present in the CA2 pyramidal layer, are never observed in the CA1 stratum pyramidale since the latter contains relatively small pyramidal cells of uniform size (Hjorth-Simonsen & Zimmer, 1975; Hjorth-Simonsen, 1977). The CA1 border with the subicular complex is clearly defined by an abrupt termination of a bundle of perforant path fibres which pass through the CA1 region (Lorento de Nó, 1934). Within this region, boundaries of the synapse-containing layer under study are also readily definable (Fig. 1c) since the extent of the stratum radiatum is limited by the stratum pyramidale on the one side and by the bundle of perforant path fibres on the other (Westrum & Blackstadt, 1962; Hjorth-Simonsen & Zimmer, 1975; Nadler *et al.*, 1980).

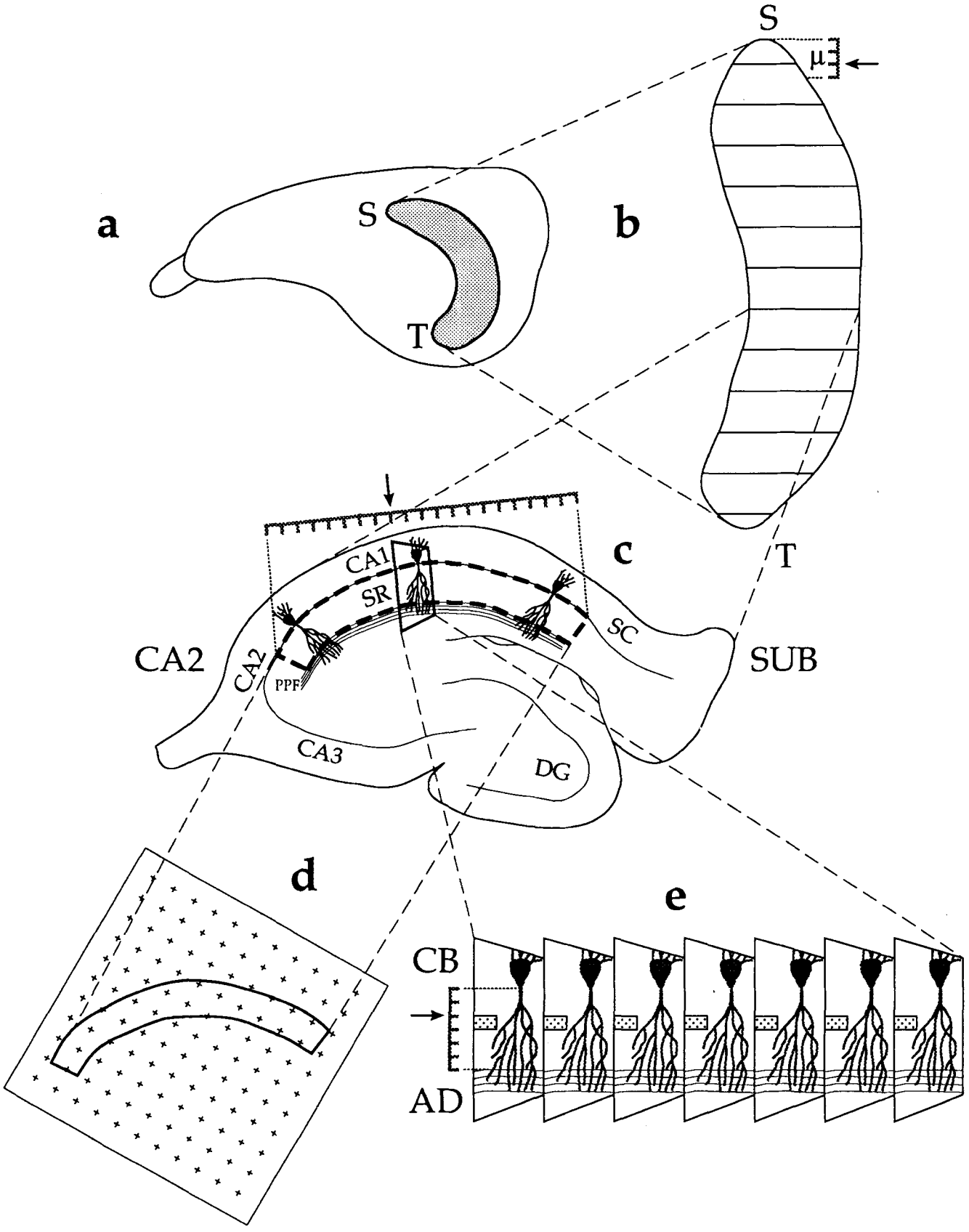
S
μ
a
S
T
b
T
c
CA1
SR
SC
CA2
CA2
PPF
SUB
CA3
DG
d
e
CB
AD

Sectional profiles of the CA1 stratum radiatum were delineated according to its boundaries specified above. Images of stained histological sections of the hippocampal formation were projected onto a table, using a projection microscope (Ken-A-Vision, Raytown, MD), and outlines of profiles of the synapse-containing layer were drawn at a final magnification of 41 ×.

Estimation of the area of synaptic layer profiles by point counting

A transparent quadratic lattice of counting points was *randomly* placed over an outline of a sectional profile of the CA1 stratum radiatum (Fig. 1d), and the number of points falling on the profile was determined. Because each point of the lattice is associated with a certain known area, the number of points hitting a given profile provides a direct and unbiased estimate of the area of sectional profiles of CA1 stratum radiatum.

A pilot experiment was carried out to determine the appropriate point density of the lattice. The guideline used was that the sampling variance of point counting should be kept at about 25% of the total intra-animal sampling variance of the sum of points (see *Nug%* in Table 2). This condition was met by choosing an interpoint distance of 10 mm relative to dimensions of profile drawings, i.e. 0.244 mm relative to actual tissue dimensions in semithin sections.

Calculation of the total volume of the synapse-containing region

The total reference volume of the CA1 stratum radiatum, $V(ref)$, was calculated with the formula: $V(ref) = \Sigma P \cdot a(p) \cdot \bar{T}$ where ΣP is the sum of lattice points hitting the entire set of stratum radiatum profiles, $a(p)$ the area associated with each point and $\bar{T}$ the average slab thickness.

Selection of fields in which to count synapses

For practical reasons, it was decided *a priori* that estimates of the synaptic numerical density in each animal would be based on an evaluation of six regional samples referred to as counting fields here. To ensure that synapses from all parts of the CA1 stratum radiatum had an equal probability of being sampled, the six counting field were distributed in a systematic random fashion. The total length of the sectional profiles of the CA1 stratum, along the CA2-subicular (CA2-SUB) axis, was measured on drawings of the histological sections used in the analysis of each animal. Since profiles of the synapse-containing layer are curved (Fig. 2), the direction of the CA2-SUB axis was approximated for a given profile by a straight line connecting the two end points of the CA1 stratum radiatum border with the stratum pyramidale (Fig. 1c). The cumulative length of the CA1 stratum radiatum along the CA2-SUB axis was calculated for an entire set of profiles and divided into six uniform intervals. The lateral sampling edge of the counting fields along the CA2-SUB axis was marked on profile drawings at these intervals after random placement within the first interval (Fig. 2, dashed lines). The markings were straight lines crossing the width of the synapse-containing layer in a direction perpendicular to the CA2-SUB axis (Fig 2). The sum of lengths of these lines gave the cumulative length of the sampled portion of the CA1 stratum radiatum along the cell body-apical dendrite (CB-AD) axis. The cumulative length determined by these measurements was also divided into six uniform intervals, and the proximal (in relation to the pyramidal cell bodies) sampling edge of the counting fields was marked on profile drawings at the defined intervals along the CB-AD axis (Fig. 2, arrows), starting with a random position within the first interval.

Preparation of serial ultrathin sections

Serial ultrathin sections of silver to pale gold interference color were prepared from the septal face of each selected slab (Fig. 1e). The first trimming cut formed the lateral sampling edge of a counting field. This cut was made in accordance with its position along the CA2-SUB axis indicated on a sectional profile drawing in relation to the surrounding blood vessels. The following trimming cuts were made so as to obtain serial ultrathin sections that had the shape of a trapezoid with its longest side formed by the first cut. The ultrathin sections spanned the entire width of the CA1 stratum radiatum, from the stratum pyramidale to the bundle of perforant path fibers. Each series of ultrathin sections was counterstained with uranyl acetate and lead citrate, mounted on a single-slot grid coated with collodion-carbon, and used to obtain electron micrographs of a counting field.

Obtaining electron micrographs of counting fields

The position of the proximal border of a counting field was

Fig. 1. Diagram illustrating stages of the sampling procedure used. (a). The left hippocampal formation (dotted area) is dissected free from its septal (S) to the temporal (T) pole. (b). The hippocampal formation is then cut, perpendicular to its septotemporal (S-T) axis, into uniform random slabs. The first cut (arrow) is placed randomly within the first inter-slab interval (μ), and the subsequent cuts are made at this interval along the entire length of the S-T axis. (c). Semithin (3 μm-thick) sections are prepared from the septal face of each plastic-embedded slab and stained with Methylene Blue. Readily observed in such sections are all subdivisions of the hippocampal formation: the dentate gyrus with its hilus (DG), fields CA3, CA2 and CA1 of the hippocampus proper, as well as the subicular complex (SC). The CA1 stratum radiatum (SR) that extends from the pyramidal cell layer to the band of perforant path fibres (PPF) is identified in each histological section. Outlines of the SR sectional profile (dashed line) are drawn with a projection microscope. The length of the SR along the CA2-subicular axis (CA2-SUB) is measured in each profile drawing as indicated by the ruler. The cumulative SR length along this axis is divided into a number of uniform random intervals to be used for placement of trimming cuts (on the block septal faces) that will form the sampling edge of ultrathin sections (arrow). (d). The area of SR sectional profiles is estimated by point counting, using profile drawings. (e). A series of consecutive ultrathin sections is prepared from the septal face of each slab. Counting fields to be photographed in an electron microscope (dotted area) are positioned in a systematic random manner along the cell body-apical dendrite axis (CB-AD) of the SR, i.e. at a certain distance from the pyramidal cell layer (arrow).

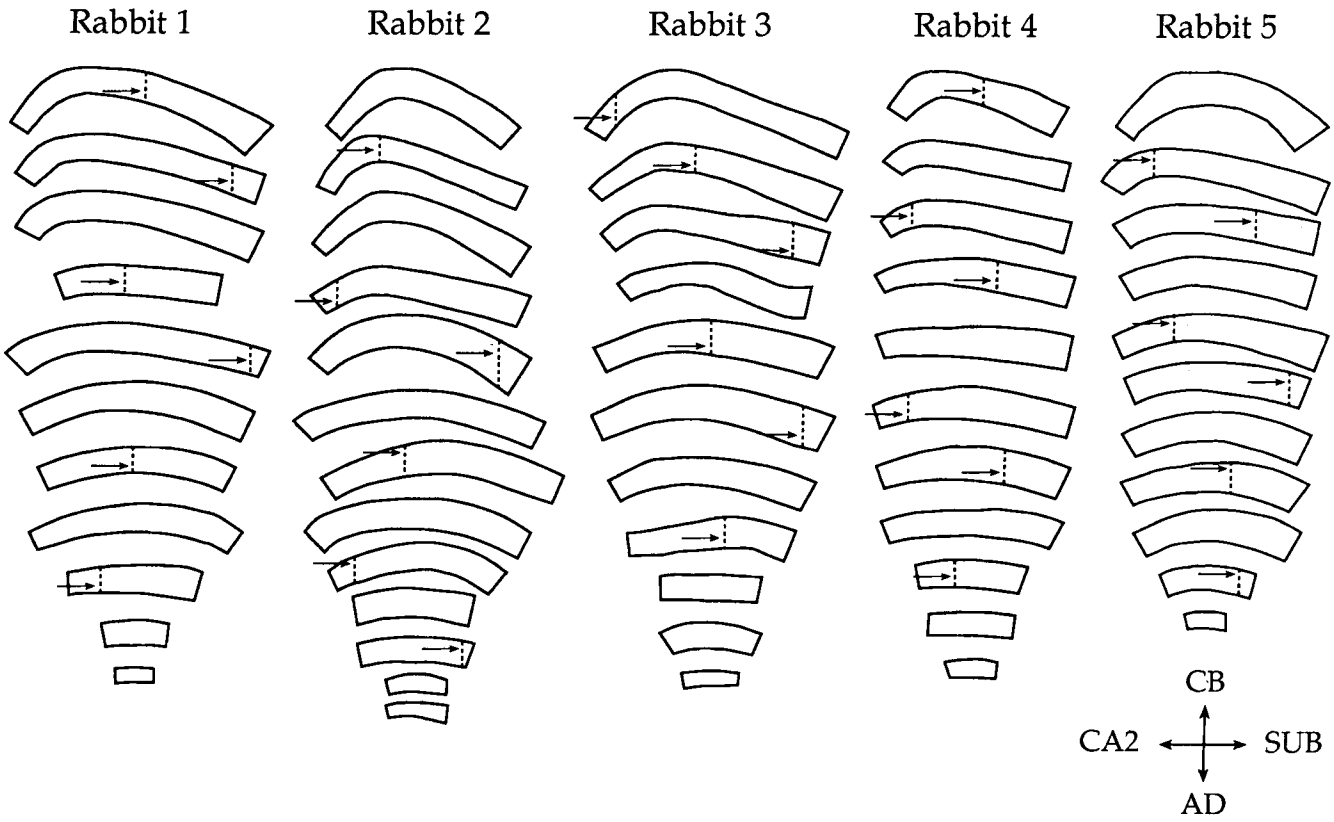

Fig. 2. Outlines of sectional profiles of the CA1 stratum radiatum (SR). For each animal under study, the entire set of profiles is shown. The outlines were drawn from projected images of stained histological sections and used to measure the SR length along the CA2-subicular (CA2-SUB) and cell body-apical dendrite (CB-AD) axes as described in the text. The direction of the axes is indicated in the right lower corner of the diagram. The cumulative length of the SR along the CA2-SUB axis was divided into six uniform random intervals that marked the lateral sampling edges (dashed lines) of the counting fields. The sum of lengths of these lines gave the SR cumulative length along the CB-AD axis. Six counting fields were placed along this axis at uniform random intervals (arrows). Note that, in this sampling scheme, the shape and orientation of the SR are irrelevant, the sampling is 2D-uniform because it is independent and systematic along two *perpendicular* axes, as indicated here and in Fig. 1. × 11.4.

determined according to its distance from the pyramidal cell layer. The distance was initially measured on the drawings of the sectional profiles and then assessed in the electron microscope with the aid of the field delineator of the microscope screen. Since a counting field had to be photographed in corresponding parts of consecutive ultrathin sections in a series, only straight ribbons of ultrathin sections were used. The sections were aligned by placing a prominent tissue landmark (such as a transversely sectioned myelinated fibre) on the same position on the microscope screen. Electron micrographs were taken at an initial magnification of 8000 × and enlarged photographically to a final magnification of 22 500 ×. At the final magnification, all synaptic contacts could be unequivocally identified and a relatively large number of synapses could be sampled. A magnification standard (grating replica) was photographed and printed with each series of electron micrographs.

Identification of synapses and their counting with disectors

The stereological disector technique (Sterio, 1984; Gundersen, 1986) was used to count synapses. Each disector consisted of two adjacent ultrathin sections, a reference section and a look-up section (Fig. 3). The postsynaptic density (PSD) was used as a counting unit. A transparency with an unbiased counting frame (Gundersen, 1977) was superimposed over a reference section micrograph (Fig. 3A). The edges of the frame and micrograph were separated by a distance (guard area) which exceeded the largest dimension of the largest PSD profile. Synapses were identified on the reference section micrograph, with the aid of micrographs of adjacent serial sections, by the presence of the PSD in a postsynaptic element and synaptic vesicles in a presynaptic axon terminal. Then synapses were labelled on the reference section micrograph if their PSD profiles were located either entirely or partly within the frame and did not intersect the forbidden edges and their extensions (Fig. 3A). Two or more profiles belonging to the same PSD of a perforated synapse (as determined by following them on consecutive sections) were connected by an imaginary straight line and treated as a single entity. Finally, only those labelled synapses that had a PSD in the reference, but not in the look-up, section were counted. Five consecutive sections were selected at random from the middle of each series for use as disector reference sections. Counts obtained from the five disectors in each of six counting fields provided samples of 219–287 synapses per animal.

Estimation of ultrathin section thickness

In order to determine the disector volume, $v(dis)$: $v(dis) = a(fr) \cdot h(dis)$, it is necessary to know the counting frame area, $a(fr)$, and the disector height, $h(dis)$, which is equal to the thickness of the reference section. The thickness of ultrathin sections was estimated with Small's method of minimal folds (Small, 1968) as described by Weibel (1979) and Royet (1991) because this method provides accurate estimates of section thickness compared with other techniques (Calverley *et al.*, 1988; De Groot, 1988; Hunter & Stewart, 1989). Minimal folds lie perpendicular to the section plane and have a width that equals twice that of the section thickness. The minimal folds were identified in ultrathin sections and photographed at a magnification of 100 000 × (the same magnification was used to photograph the standard grating replica). The fold width was measured directly on the negatives. In all of the series of ultrathin sections that were examined, there were sections that did not contain minimal folds. The mean section thickness of all those sections that contained minimal folds was used to calculate the height of the disectors, $h(dis)$.

Calculation of synaptic numerical density per unit volume

The numerical density of synapses per unit volume, N_V, was calculated for each animal with the formula: $N_V = \bar{Q}^- / \bar{v}(dis)$. In this formula, $\bar{Q}^-$ is the mean number of synapses counted per disector and $\bar{v}(dis)$ the mean disector volume.

Calculation of the total number of synapses in the total volume of the synapse-containing region

The total number of synapses, $N(syn)$, in the total reference volume of the synapse-containing layer, $V(ref)$, was calculated for each animal with the formula:

$$N(syn) = V(ref) \cdot N_V = V(ref) \cdot \frac{\bar{Q}^-}{\bar{v}(dis)}$$

A general requirement of the two step procedure employed for estimating the $N(syn)$ is that the processed volume of the specimens used to estimate $V(ref)$ and that used to estimate N_V must correspond to each other. Even though ultrathin sections may stretch, no plastic-embedded tissue is ever lost from the sections, and the volume of disectors, $\bar{v}(dis)$, formed by ultrathin sections can be directly related to the volume of the synapse-containing layer, $V(ref)$, estimated with point counting on semithin sections.

Estimation of sampling variances

Stereological sampling of synapses involves a hierarchy of sampling levels, including (1) disectors and counting points, (2) counting fields and semithin sections, (3) individual animals and (4) groups of animals. In order to evaluate the appropriateness of the sampling scheme, it is necessary to estimate the variance contribution from all sampling levels to the total group variation among individual animals. This can be done according to well known statistical principles (Gundersen & Jensen, 1987). For two adjacent sampling levels, the observed relative variance, OCV_j^2, at a higher, j th, level is the sum of the expected relative variance, CV_j^2, at that level and the observed relative variance of the mean at the level below, OCE_{j-1}^2:

$$OCV_j^2 = CV_j^2 + OCE_{j-1}^2 \quad (1)$$

These variances are relative since they are related to the means: both the coefficient of variation, CV, and the coefficient of error, CE, can be conventionally expressed as $CV = \text{SD}/\text{mean}$ (where SD is the standard deviation) and $CE = \text{SEM}/\text{mean}$ (where SEM is the standard error of the mean). Stereological sampling at a lower level should be terminated when the computable variance of a stereological estimate at this level, OCE_{j-1}^2, is about half or less than the total variance at the higher level, OCV_j^2, i.e. when the CV_j^2 contributes most to the observed variation at the higher level. When the contribution to the total observed variance from each sampling level is known, it is possible to optimize the sampling scheme (e.g., the most efficient way to improve the precision of stereological estimates is to increase the amount of sampling at the level that contributes most to the overall variance).

As indicated above, the compound estimator of the total synapse number, $N(syn)$, is the product of two variables, the number of synapses per unit volume, N_V, and the total reference volume, $V(ref)$. Because constants related to sampling intensities (point density, disector volume) have no effect on the relative variance of $N(syn)$, the variances of N_V and $V(ref)$ can be substituted by those of $\bar{Q}^-$ and ΣP, respectively. Accordingly, the variance of $N(syn)$ can be estimated as $Rel\ Var[N] = Rel\ Var[\bar{Q}^- \cdot \Sigma P]$*.

Tables 2, 3 and 4 show formulas for calculating sampling variances. Although the sampling variances are themselves estimates, they can be used to get a feeling as to whether the stereological sampling was performed with an appropriate degree of precision. For symbols of the variances (CE^2 and CV^2), prefixes E and O denote terms of expected and observed variation, respectively, while suffixes a, f, s and p indicate that the variance is estimated for animals, fields used to count synapses, histological sections and point counting, respectively. Some variances were calculated in a special way as described below.

Because a systematic random sample of sections was used to assess the ΣP parameter, sampling variances of ΣP were estimated with formulas (Gundersen & Jensen, 1987) that differ from those that are conventionally used on independent random samples. The expected variance of point counting with a lattice of systematic points on n_s sections, referred here to as the nugget variance, Nug, was calculated with the formula:

$$Nug = 0.0724 \cdot (b/\sqrt{a}) \cdot \sqrt{n_s \cdot \Sigma P}$$

In this formula, the value 0.0724 is a constant for point lattices with a quadratic arrangement and $b/\sqrt{a}$ is an average shape factor for a set of sectional profiles, i.e. the length of the

* When evaluating the variance of the product $V(ref) \cdot N_V$, one needs to take into account the variance of both parameters and their co-variance at the level of animals. In this study, the co-variance was relatively small and has been ignored. This may not necessarily be the case in other synapse-containing regions and should be taken into account as described by Kroustrup and Gundersen (1983) and Pakkenberg and Gundersen (1988).

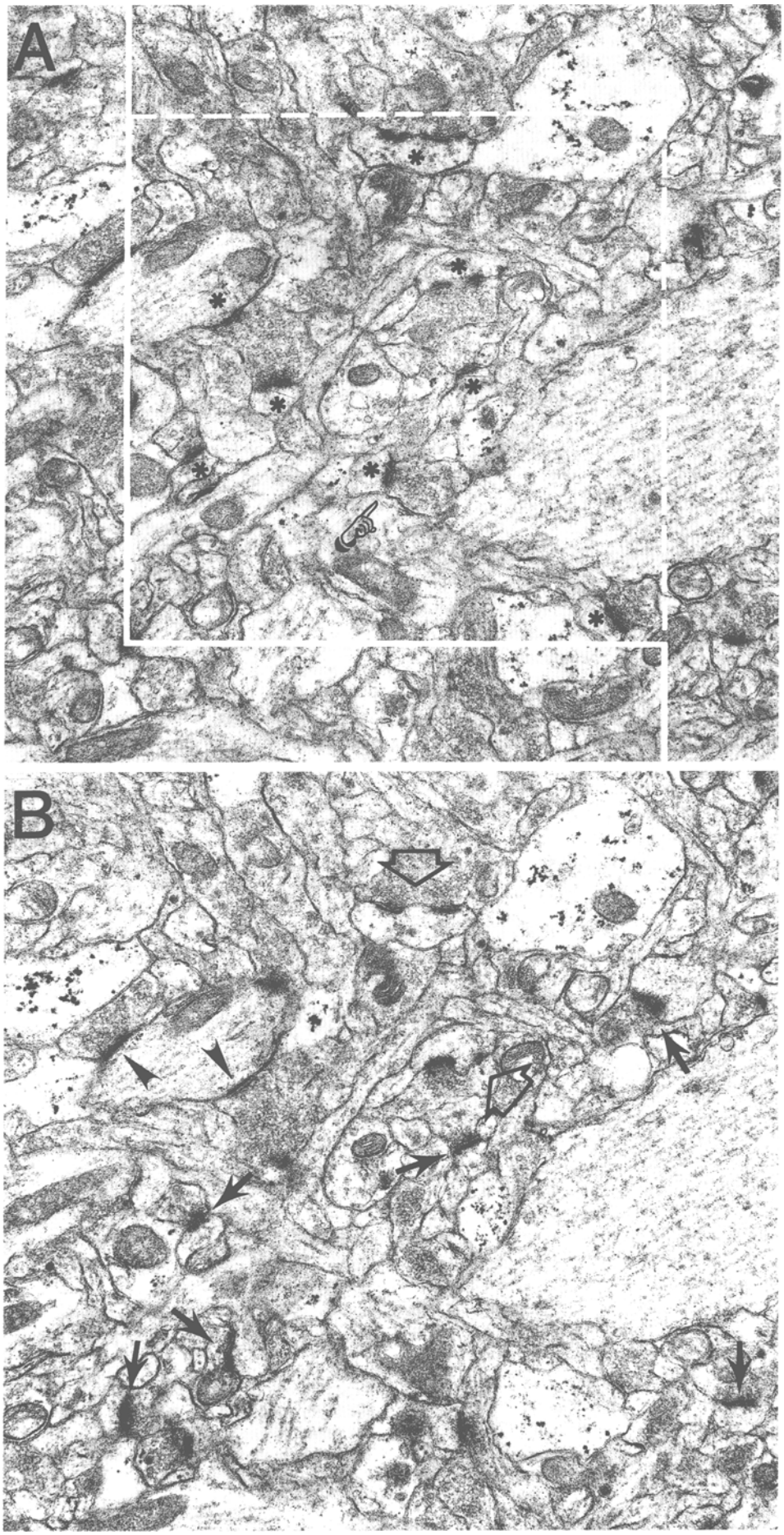
A
B

Table 1. Estimates of the total reference volume, synapse density (number per unit volume) and total number of synapses in the total reference volume of the rabbit CA1 stratum radiatum.

Parameter	*Rabbit 1*	*Rabbit 2*	*Rabbit 3*	*Rabbit 4*	*Rabbit 5*	*Group mean*
Total reference volume: $V(ref) = \Sigma P \cdot a(p) \cdot \bar{T}$	17.0	20.9	17.4	14.2	18.4	$17.6\,mm^3$
Coefficient of variation of $V(ref)$: $OCV_a[V(ref)]$						0.14
Synaptic numerical density: $N_V = \bar{Q}^-/\bar{v}(dis)$	1.40	1.38	1.56	1.31	1.19	$1.37 \times 10^9\,mm^{-3}$
Coefficient of variation of N_V : $OCV_a[N_V]$						0.10
Total number of synapses in the total reference volume: $N(syn) = V(ref) \cdot N_V$	2.38	2.88	2.71	1.86	2.19	2.40×10^{10}
Coefficient of variation of $N(syn)$: $OCV_a[N(syn)]$						0.17

The observed coefficient of variation, *OCV*, was calculated for each parameter under study with the formula: $OCV = OSD/Mean$ where *OSD* is the observed standard deviation ($OSD_a[V(ref)] = 2.42\,mm^3$; $OSD_a[N_V] = 0.14 \times 10^9\,mm^{-3}$; $OSD_a[N(syn)] = 0.41 \times 10^{10}$) and *Mean* is the estimated group mean.

profile boundary, b, divided by the square root of the profile area, $\sqrt{a}$. Profile shapes are most conveniently expressed by the dimensionless ratio, $b/\sqrt{a}$, which has a minimum of $2\sqrt{\pi} = 3.54$ for a circle (Gundersen & Jensen, 1987).

The shape factor can be estimated by comparing the overall shape of sectional profiles with those presented in a nomogram that predicts the number of points necessary to perform counts (Gundersen & Jensen, 1987; see Fig. 18 for the nomogram). Alternatively, the shape factor can be derived from the boundary length and area assessed with a lattice of test lines (Gundersen & Jensen, 1987) or measured with an image analysis system. The latter approach was employed in the present study. Actual shapes of sectional profiles of the CA1 stratum radiatum are shown in Fig. 2. The $b/\sqrt{a}$ ratio was assessed for each profile by tracing its outlines with a digitizing tablet, and the resulting values were used to calculate the average $b/\sqrt{a}$ ratio for the entire set of profiles in each animal.

The variance of profile areas among the systematic random sample of histological sections used to estimate $V(ref)$, i.e. $Var[\Sigma a]$, was computed with the formula:

$$Var[\Sigma a] = [3(A - Nug) - 4B + C]/12 \qquad (2)$$

where $A = \Sigma(P_i \cdot P_i)$, $B = \Sigma(P_i \cdot P_{i+1})$ and $C = \Sigma(P_i \cdot P_{i+2})$. Explicit examples of such calculations are available in the literature (Pakkenberg & Gundersen, 1988; Brændgaard *et al.*, 1990; West & Gundersen, 1990).

The statistical model outlined above is applicable only to those cases of systematic random sampling in which the sampling is performed along a single axis of a given region. Although synapses were also sampled in a systematic random manner, such sampling was carried out along two axes of the synapse-containing layer. The third axis was effectively sampled randomly. Statistical models defining variances for a systematic sampling design of this kind are not available. Therefore, sampling variances of $\bar{Q}^-$ were conservatively calculated as conventional variances for independent variables. Estimated separately at lower sampling levels, variances of ΣP and $\bar{Q}^-$ were then used to calculate the variance of N at the level of individual animals.

Results

Characterization of the synaptic population of the rabbit CA1 stratum radiatum

Examination of electron micrographs of the CA1 stratum radiatum showed that the synaptic population of this region is morphologically heterogeneous. It includes two basic categories of synapses: axodendritic contacts involving dendritic shafts and axospinous ones involving dendritic spines (Fig. 3B). The latter category can be further subdivided into perforated and nonperforated synapses that exhibit discontinuous or continuous PSDs, respectively (Fig. 3B). Counts performed with a total of 30 disectors per animal provided samples of 5–12 axodendritic, 23–48 axospinous perforated and 191–228 axospinous nonperforated synapses. If the present study were aimed at a differential quantitative analysis of these synaptic types, it would have been necessary to count axodendritic and axospinous perforated junctions with a

Fig. 3. Electron micrographs of two consecutive ultrathin sections through the CA1 stratum radiatum of the rabbit hippocampus demonstrating the application of the disector method for synapse counting. The disector is formed by a reference section (A) and a look-up section (B). The unbiased counting frame of Gundersen (1977) indicated by white lines is randomly placed over the reference section micrograph. The postsynaptic density (PSD) is used as a counting unit. Synapses are counted with the disector if their PSD is not seen in the look-up section, but is observed in the reference section being positioned within the counting frame or intersected by its inclusion edges (broken lines) and not by the exclusion edges or their extensions (solid lines). Analysis of the micrographs presented here shows that only one synapse (pointing finger) among those that have their PSD within the counting frame (asterisks) can be counted according to the disector counting rule. Note that various types of synaptic contacts are encountered in the CA1 stratum radiatum, including axodendritic (arrowhead), axospinous perforated (open arrows) and axospinous nonperforated (closed arrows) synapses (B). ×21 500.

Table 2. Stereological sampling variances of the total reference volume, $V(ref)$, and primary parameters used to calculate the variances and $V(ref)$.

Parameter	*Rabbit 1*	*Rabbit 2*	*Rabbit 3*	*Rabbit 4*	*Rabbit 5*	*Group mean*
Number of histological sections, n_s	11	13	11	11	11	
Sum of points over all sections, ΣP	160	185	158	140	168	
Area associated with each point (mm^2), a, (p)	0.0595	0.0595	0.0595	0.0595	0.0595	
Mean thickness of tissue slabs (mm), $\bar{T}$	1.79	1.90	1.85	1.70	1.84	
Variance of point counting or Nugget effect, Nug:						
$Nug = 0.0724 \cdot (b/\sqrt{a}) \cdot \sqrt{n_s \cdot \Sigma P}$	18.2	21.2	17.9	15.9	17.5	
Shape factor, $b/\sqrt{a}$	5.98	5.96	5.94	5.59	5.61	
Coefficient of error squared of point counting:						
$ECE_p^2[\Sigma P] = Nug/(\Sigma P)^2$	0.0007	0.0006	0.0007	0.0008	0.0006	0.0007
Variance of sectional profile areas, $Var[\Sigma a]$:						
$Var[\Sigma a] = [3(A - Nug) - 4B + C]/12$	53.6	67.4	52.7	41.4	40.0	
$A = \Sigma(P_i \cdot P_i)$	2784	3125	2738	2048	2862	
$B = \Sigma(P_i \cdot P_{i+1})$	2458	2787	2404	1821	2574	
$C = \Sigma(P_i \cdot P_{i+2})$	2178	2645	2088	1684	2242	
Coefficient of error squared of Σa among sections: $ECE_s^2[\Sigma a] = Var[\Sigma a]/(\Sigma P)^2$	0.0021	0.0020	0.0021	0.0021	0.0014	0.0019
Total intra-animal variance of ΣP, $Var[\Sigma P]$:						
$Var[\Sigma P] = Nug + Var[\Sigma a]$	71.8	88.6	70.6	57.3	57.5	
$Nug\% = (Nug \cdot 100)/Var[\Sigma P]$	25%	24%	25%	28%	30%	
Total intra-animal coefficient of error squared of ΣP:						
$OCE_a^2[\Sigma P] = Var[\Sigma P]/(\Sigma P)^2$	0.0028	0.0026	0.0028	0.0029	0.0020	0.0026
Total intra-animal coefficient of error of V_{ref}: $OCE_a[\Sigma P]$	0.053	0.051	0.053	0.054	0.045	0.051

Note that the variances of $V(ref)$ below the group sampling level were estimated as variances of the sum of points, ΣP.

larger number of disectors in order to obtain representative samples of at least 100 synapses of a given type per animal.

Estimates of the reference volume and their sampling variances

The data obtained are summarized in Tables 1 and 2. The mean total volume of the synapse-containing layer, $V(ref)$, was estimated to be 17.6 mm^3 for the group of animals studied, with a range of 14.2–20.9 mm^3. The observed coefficient of variation of the $V(ref)$ among individual animals ($OCV_a[V(ref)]$) was equal to 0.14. Most of this variation (87%) was due to the inherent biological variability of $V(ref)$ among animals. The overall contribution of the variances associated with stereological sampling ($ECE_s^2[\Sigma a] + ECE_p^2[\Sigma P] = 0.0026$) to the total group variance of $V(ref)$ ($OCV_a^2[V(ref)] = 0.0196$) amounted to only 13%. The precision of individual $V(ref)$ estimates, expressed as the total intra-animal coefficient of error of ΣP ($OCE_s[\Sigma P]$) and averaged over all animals, was 5.1%.

Table 3. Stereological sampling variance of the synaptic numerical density, N_V, and primary parameters used to calculate the variance and N_V.

Parameter	*Rabbit 1*	*Rabbit 2*	*Rabbit 3*	*Rabbit 4*	*Rabbit 5*	*Group mean*
Mean volume of disectors (μm^3): $\bar{v}(dis) = \bar{a} \cdot \bar{t}$ (mean counting frame area $\bar{a} = 64\,\mu m^2$; mean thickness of ultrathin sections $\bar{t} = 0.096\,\mu m$)	6.14	6.14	6.14	6.14	6.14	
Total number of synapses counted with $n_d = 30$ disectors	258	254	287	242	219	
Mean number of synapses counted per disector, $\bar{Q}^-$	8.60	8.47	9.57	8.07	7.30	
Total intra-animal variance of $\bar{Q}^-$ among $n_f = 6$ counting fields: $OSD_f^2[\bar{Q}^-]$	1.33	1.72	2.47	2.07	3.50	
Total intra-animal coefficient of error squared of $\bar{Q}^-$ among counting fields: $OCE_f^2[\bar{Q}^-] = OSD_f^2[\bar{Q}^-]/(\bar{Q}^{-2} \cdot n_f)$	0.0030	0.0040	0.0045	0.0053	0.0109	0.0055
Total intra-animal coefficient of error of N_V: $OCE_f[\bar{Q}^-]$	0.055	0.063	0.067	0.073	0.104	0.072

Note that the variance of N_V was estimated, below the group sampling level, as variance of the mean number of synapses, $\bar{Q}^-$, counted per disector.

Table 4. Stereological sampling variance of the total synapse number, $N(syn)$, and its contribution to the total group variance of $N(syn)$.

Parameter	*Rabbit 1*	*Rabbit 2*	*Rabbit 3*	*Rabbit 4*	*Rabbit 5*	*Group mean*
Total intra-animal coefficient of error squared of N: $OCE_a^2[N] = OCE_f^2[\bar{Q}^-] + ECE_s^2[\Sigma a] + ECE_p^2[\Sigma P]$	0.0058	0.0066	0.0073	0.0082	0.0129	0.0082
Contribution of the $OCE_a^2[N]$ to the $OCV_a^2[N(syn)]$: $OCE_a^2[N]\% = (OCE_a^2[N] \cdot 100)/OCV_a^2[N(syn)]$						28%
Total intra-animal coefficient of error of $N(syn)$: $OCE_a[N]$	0.076	0.081	0.085	0.091	0.114	0.089

Note that the relative variance of $N(syn)$ was estimated, below the group sampling level, as $Var[N] = Var[\bar{Q}^- \cdot \Sigma P]$.
Values of the $OCE_f^2[\bar{Q}^-]$, $ECE_s^2[\Sigma a]$ and $ECE_p^2[\Sigma P]$ are presented in Tables 2 and 3. For the $OCV_a^2[N(syn)]$ value see Table 1.

Estimates of synaptic numerical density and their sampling variances

The data are shown in Tables 1 and 3. Estimates of synaptic numerical density obtained from individual animals were in the range of $1.19–1.56 \times 10^9$ mm^{-3} which provided a group mean value of 1.37×10^9 mm^{-3}. The observed coefficient of variation of N_V among animals in the group, $OCV_a[N_V]$ (calculated as the $OCV_a^2[V(ref)]$ above), was equal to 0.10. The lowest level of synapse sampling was that of counting fields and not of disectors since synapses were sampled with five dissectors from the same counting field. The contribution of the variance associated with stereological sampling ($OCE_f^2[\bar{Q}^-] = 0.0055$) to the total group variance of N_V ($OCV_a^2[N_V] = 0.0100$) reached 55%, while the rest of the contribution (45%) came from the inherent biological variation among animals. The precision of individual N_V estimates ($OCE_f[\bar{Q}^-]$) had a value of 7.2% when averaged over all animals studied.

Estimates of the total number of synapses and their sampling variances

The data are presented in Tables 1 and 4. The total number of synapses in the total volume of the CA1 stratum radiatum, $N(syn)$, was estimated to be 2.38, 2.88, 2.71, 1.86 and 2.19×10^{10} for the animals under study, the group mean being equal to 2.40×10^{10}. The coefficient of variation for the group was 0.17. Analysis of sampling variances of $N(syn)$ demonstrated that the variation associated with stereological sampling ($OCE_a^2[N] = 0.0082$) accounted for 28% of the overall group variation ($OCE_a^2[N(syn)] = 0.0289$). Individual estimates of $N(syn)$ had a precision ($OCE_a[N]$) of 8.9%.

Discussion

Over the past four decades, numerous attempts were made to estimate the number of synapses in various regions of the central nervous system. Most of the previous studies, however, were hampered by the use of two-dimensional stereological techniques. Designed to convert profile counts made in two-dimensional images of sections into the number of three-dimensional objects, these techniques rely on assumptions about the size, shape and orientation of objects. Most assumptions made with regard to synapses were unrealistic (e.g., synaptic contacts were assumed to fit the model of flat circular discs having the same diameter) which resulted in biases (De Groot, 1986). The effects of these potential biases on the results of synapse counts are difficult, if not impossible, to evaluate in practice. This makes the data available in the literature virtually uninterpretable. There is a need, therefore, to reevaluate the reported results of synapse quantitation with unbiased stereological approaches. Such a goal can be achieved by using the proposed method since it provides estimates of the total synapse number that are unbiased and are not affected by changes in tissue volume. This method is based on principles of modern stereology and utilizes recently developed sampling and counting techniques that are assumption-free and therefore bias-free. The advantages of the method described here as opposed to conventional stereological techniques are discussed below.

Estimating total synapse number, rather than synaptic numerical density

One of the most important features of the proposed method is that it is designed to provide estimates of the *total* number of synapses, whether they exemplify the entire synaptic population or certain morphological subtypes in a neuroanatomically defined region. Here, the key word is *total*, for without information about total synapse number, it is not possible to draw conclusions with regard to changes in the quantity of synaptic contacts under experimental or pathological conditions. For example, the conclusions of many of the earlier studies of age-related synapse loss were based on numerical density data (Geinisman *et al.*, 1995). Age-related reductions in synaptic numerical densities, however, cannot be unambiguously interpreted as evidence of synapse loss, in that they can result from changes in either the volume of the region, or synapse number or both. Estimating total synapse

number, rather than synaptic numerical density, eliminates the questionable assumption, implicit in comparisons of density data, that the volumes of the regions being compared are the same (Brændgaard & Gundersen, 1986; Swaab & Uylings, 1987; Oorschot, 1994).

Sampling synapses in a uniform, rather than in a non-uniform, fashion

The sampling strategy of the earlier studies was to sample synapses from a certain typical portion of a brain region of interest. The results obtained from this selective sampling cannot be extrapolated to the entire region and conclusions can be drawn only with respect to the particular portion examined. In contrast, the sampling procedure implemented in this study probes the entire synapse-containing region. This procedure provides systematic random samples of both histological sections and synapses to be used for estimating the total reference volume and synaptic numerical density, respectively. The reference volume is assessed according to the Cavalieri principle (Gundersen & Jensen, 1987; Michel & Cruz-Orive, 1988), using parallel histological sections that are taken at a uniform random interval along one axis of a synapse-containing region. Synapses are sampled with an equal probability along all three axes of a given region. In the region examined in this study, fields in which to count synapses are positioned randomly along the septo-temporal axis (due to a random placement of cuts used to make tissue slabs) and in a systematic random manner along the other two axes (CA2-SUB and CB-AD) of the CA1 stratum radiatum (Fig. 1). This sampling paradigm is unbiased in that it ensures that all parts of the synapse-containing region, as well as all synapses within the region, have an equal chance of being sampled.

Counting synapses with three-dimensional, rather than with two-dimensional, probes

The counting procedure of conventional stereology employs single, non-serial sections as a counting probe. There are some inherent problems in this approach. One of them is that a single section is a two-dimensional probe with which objects are sampled with a probability that is proportional to the their linear dimension in the plane perpendicular to that of the section. This fundamental property of two-dimensional counting probes explains why objects have more chances of being counted in single sections when their dimensions are relatively large or when they are sectioned perpendicular, rather than parallel, to their long axis. It is obvious, therefore, that the results of object counts in single sections depend on the size, shape and orientation of a given counting unit (e.g., the postsynaptic density or synaptic apposition zone in the case of synapses). Other factors that determine the probability with which objects are counted in single sections include the section thickness, truncation (also known as the phenomenon of lost caps, i.e. fragments that actually or apparently disappear from the cut surface of sections) and overprojection (also known as Holmes' effect, i.e. an enlargement of opaque profile images due to the finite thickness of transparent sections). In the present study, the disector technique was used to count synapses. The disector is a three-dimensional stereological probe designed to directly count objects, not their profiles, in three-dimensional space. Consequently, counts made with the disector according to the unbiased counting rule are unaffected by the biases characteristic of the conventional stereological approaches (Sterio, 1984; Gundersen, 1986).

Identifying synapses in serial, rather than in single, ultrathin sections

The only requirement of the disector method is that the objects counted with the disector be unambiguously identifiable on the sections (Gundersen, 1986). In the case of synapse counting, this requirement is fulfilled by examining micrographs of consecutive serial sections where all profiles produced by sectioning of a synaptic contact can be readily identified. In contrast, this cannot be achieved by using two-dimensional counting probes, i.e. single sections, for synapse quantitation. The criterion, which is generally employed for the identification of synapses in tissue treated with osmium tetroxide, is the presence of synaptic vesicles in a presynaptic axon terminal and the presence of a PSD in a postsynaptic element. Examination of synaptic contacts in electron micrographs of consecutive serial sections has revealed, however, that synapses can exhibit individual sectional profiles that completely lack either synaptic vesicles or a PSD (Geinisman *et al.*, 1991). When encountered in a single section, such a structure cannot be classified as a synaptic profile. Moreover, small or tangentially cut synapses cannot be reliably recognized in a single section due to a negligible size of their profiles (Curcio & Hinds, 1983; deToledo-Morrell *et al.*, 1988). As a consequence of this, the synaptic numerical density is systematically underestimated by as much as 20% (Curcio & Hinds, 1983). These difficulties are compounded by the presence of perforated synapses, including those with a segmented PSD, in many regions of the central nervous system (Calverley & Jones, 1990). A perforated synapse can be erroneously identified in a single section as two or more nonperforated ones (De Groot & Bierman, 1983) or not identified at all if the section passes through the interval between separate PSD segments (Geinisman *et al.*, 1987). Thus, an unambiguous identification of synapses, which is a prerequisite for obtaining unbiased estimates of their number, can only be

performed with the aid of consecutive serial sections. Since serial ultrathin sections have to be prepared for the purpose of synapse identification, it does not make sense to count synaptic profiles in a single section(s) from a series and then to transform the profile counts into synapse number with conventional stereological techniques that are known to be biased. Having serial ultrathin sections prepared, it is possible to count synapses directly with the disector formed by a section pair(s) selected from a series.

Evaluating the precision of stereological estimates of the total synapse number

Since the sampling and counting procedures employed in this work are unbiased, they provide *estimates of the true total number* of synapses. The extent to which such stereological estimates deviate from the true value depends only on their precision. The precision is most conveniently expressed by the coefficient of error (CE) of individual estimates which is a measure of the total intra-individual variation associated with stereological sampling (West & Gundersen, 1990). Computation of the observed coefficients of error (OCE_a) from the data reported here indicate that the individual estimates of $V(ref)$, N_V and $N(syn)$ were obtained with a precision of 5.1, 7.2 and 8.9%, respectively (Tables 2, 3 and 4). Although such precision can be improved by additional stereological sampling, the contribution of the intra-animal variation associated with stereological sampling ($OCE_a^2[N]$) to the total group variance of $N(syn)$, $OCV2_a[N(syn)]$, was equal to 28% (Table 4). Therefore, it is the inherent biological variability among animals that contributed most to the total group variance of the estimates made with the sampling scheme used here.

Predicting group sizes in studies involving group comparisons

Studies on synapse quantitation are most frequently aimed at determining whether or not groups of animals or individuals differ from each other with respect to the number of synaptic contacts in a given region of the nervous system. An obvious way to increase the probability of demonstrating a statistically significant difference between group means is to reduce the variances of the means. The observed variance of the group mean is the sum of the variability resulting from stereological sampling and that stemming from the biological inter-individual variability. If the former factor contributes most to the variance of the group mean, this variability can be more efficiently reduced by increasing the amount of stereological sampling. If, on the contrary, the latter factor is the major contributor to the variance of the group mean, the most efficient way to reduce the variance is to increase the group size.

Based on the above considerations, the appropriate option for optimizing the sampling design of the present work would be to examine more animals in the group, rather than to improve the precision of individual stereological estimates. The decision of how many animals need to be examined in the group can be made with the t statistic that takes the following form:

$$t = \frac{\text{difference between observed group means } [N(syn)]}{\text{standard error of difference}}$$

$$2.3 < \frac{20\% \text{ of group mean } [N(syn)]}{\sqrt{2 \cdot OSD_a^2[N(syn)]/n}}$$

$$2.3 < \frac{0.48}{\sqrt{(0.41^2 + 0.41^2)/n}}$$

$$n \geq 8 \qquad (3)$$

For these calculations, the data obtained from only one group of animals were available. The variance of $N(syn)$ for the other group was presumed to be the same. Difference between group means was set at 20% since a change of this magnitude in the total number of synapses is most likely to have functional consequences. The statistic shows that, with the variances observed here (i.e., with the described sampling scheme), it is necessary to examine a minimum of 8 animals per group in order to demonstrate that group mean differences of 20% are significant at the 0.05 level.

Although the sampling design used here is close to being optimal, it can be further optimized for group comparisons by increasing the number of animals per group to 8 and the number of counting fields to 7 or 8. The purpose of the latter modification is related to the data showing that the intra-animal variance of N_V associated with stereological sampling, $OCE_f^2[\bar{Q}^-]$, constitutes 55% of the total observed inter-animal variance of N_V, $OCV_a^2[N_V]$. Additionally, the number of disectors per counting field can be decreased to about 3 which would reduce the workload at this level. The discussion of the above underlines the design-based nature of the methodology described and its importance in the planning of quantitative morphological studies.

Conclusions

The biologically important information from this study consists of two numbers presented in Table 1: the mean number of synapses in CA1 stratum radiatum of young female rabbits, $N(syn) = 2.40 \times 10^{10}$; and the observed variability of that estimate among five rabbits, $OCV_a[N(syn)] = 0.17$. Of secondary interest is the number presented in Table 4: the stereological uncertainty or error, which indicates that only 28% of the total variance of the $N(syn)$ estimate observed

in the group can be attributed to the estimation procedure itself and that the sampling scheme is appropriate.

Most of this paper is devoted to describing how one actually designs a uniform random sampling scheme of the entire stratum radiatum. Three features of this scheme: uniform sampling at all levels, three-dimensional counting, and inclusion of the entirety of CA1 striatum radiatum ensure that the estimate, $N(syn) = 2.40 \times 10^{10}$, is unbiased. Only the computations shown in Table 1 are needed to derive this estimate. The descriptions and discussions of the rationale for the sampling protocol used and the somewhat complicated computations required for an evaluation of the variances in the multilevel sampling scheme are not of biological importance and are presented for two major reasons. One of these is to demonstrate that the $CE[N(syn)]$ of 0.089 is a mere 28% of the total variance of the $N(syn)$ estimate. The other reason is to illustrate practical ways of reducing the variation associated with stereological sampling so that its background noise would not obscure the actual results of synapse quantitation.

In conclusion, it needs to be emphasized that the method proposed here can be applied to the study of any type of synapse, such as the axodendritic, axospinous or axosomatic one, and of any defined region of the nervous system. Being generally applicable, completely unbiased and design-based, the proposed method provides a valuable tool for obtaining reliable estimates of the total number of synapses in various distinct regions of the nervous system.

Acknowledgments

We thank William Goossens for his skillful technical help. This work was supported by the grant NS34582 from the NINDS and the ADRC at Johns Hopkins University.

References

BRÆNDGAARD, H. & GUNDERSEN, H. J. G. (1986) The impact of recent stereological advances on quantitative studies of the nervous system. *Journal of Neuroscience Methods* **18**, 39–57.

BRÆNDGAARD, H., EVANS, S. M., HOWARD, C. V. & GUNDERSEN, H. J. G. (1990) The total number of neurons in the human neocortex unbiasedly estimated using optical disectors. *Journal of Microscopy* **157**, 285–304.

CALVERLEY, P. K. S. & JONES, D. G . (1990) Contribution of dendritic spines and perforated synapses to synaptic plasticity. *Brain Research Reviews* **15**, 215–49.

CALVERLEY, P. K. S., BEDI, K. S. & JONES, D. G. (1988) Estimation of the numerical density of synapses in rat neocortex. Comparison of the 'disector' with an 'unfolding' method. *Journal of Neuroscience Methods* **23**, 195–205.

COGGESHALL, R. E. & LEKAN, H. A. (1996) Methods for determining numbers of cells and synapses: a case for more uniform standards of review. *Journal of Comparative Neurology* **364**, 6–15.

CURCIO, C. A. & HINDS, J. W. (1983) Stability of synaptic density and spine volume in dentate gyrus of aged rats. *Neurobiology of Aging* **4**, 77–87.

DE GROOT, D. M. G. (1986) A critical evaluation of methods for estimating the numerical density of synapses. *Journal of Neuroscience Methods* **18**, 79–101.

DE GROOT, D. M. G. (1988) Comparison of methods for the estimation of the thickness of ultrathin tissue sections. *Journal of Microscopy* **151**, 23–42.

DE GROOT, D. M. G. & BIERMAN, E. P. B. (1983) The complex-shaped 'perforated' synapse, a problem in quantitative stereology of the brain. *Journal of Microscopy* **131**, 355–60.

DETOLEDO-MORRELL, L., GEINISMAN, Y. & MORRELL, F. (1988) Individual differences in hippocampal synaptic plasticity as a function of aging: behavioral, electrophysiological and morphological evidence. In *Neural Plasticity: A Lifespan Approach* (edited by PETIT, T. L. & IVY, G.) pp. 283–328. New York: Liss.

GAARSKJAER, F. B. (1978) Organization of the mossy fiber system of the rat studied in extended hippocampi. I. Terminal area related to number of granule and pyramidal cells. *Journal of Comparative Neurology* **178**, 49–72.

GEINISMAN, Y., MORRELL, F. & DETOLEDO-MORRELL, L. (1987) Axospinous synapses with segmented postsynaptic densities: a morphologically distinct synaptic subtype contributing to the number of profiles of 'perforated' synapses visualized in random sections. *Brain Research* **423**, 179–88.

GEINISMAN, Y., DETOLEDO-MORRELL, L. & MORRELL, F. (1991) Induction of long-term potentiation is associated with an increase in the number of axospinous synapses with segmented postsynaptic densities. *Brain Research* **566**, 77–88.

GEINISMAN, Y., DETOLEDO-MORRELL, L., MORRELL, F. & HELLER, R. E. (1995) Hippocampal markers of age-related memory dysfunction: behavioral, electrophysiological and morphological perspectives. *Progress in Neurobiology* **45**, 223–52.

GUNDERSEN, H. J. G. (1977) Notes on the estimation of the numerical density of arbitrary profiles: the edge effect. *Journal of Microscopy* **111**, 219–23.

GUNDERSEN, H. J. G. (1986) Stereology of arbitrary particles. A review of unbiased number and size estimators and the presentation of some new ones, in memory of William R. Thompson. *Journal of Microscopy* **143**, 3–45.

GUNDERSEN, H. J. G. & JENSEN, E. B. (1987) The efficiency of systematic sampling in stereology and its prediction. *Journal of Microscopy* **147**, 229–63.

GUNDERSEN, H. J. G., BAGGER, P., BENDTSEN, T. F., EVANS, S. M., KORBO, L., MARCUSSEN, N., MØLLER, A., NIELSEN, K., NYENGAARD, J. R., PAKKENBERG, B., SØRENSEN, F. B., VESTERBY, A. & WEST, M. J. (1988a) The new stereological tools: disector, fractionator,

nucleator and point sampled intercepts and their use in pathological research and diagnosis. *Acta Pathologica Microbiologica and Immunologica Scandinavica* **96**, 857–81.

HJORTH-SIMONSEN, A. (1977) Distribution of commissural afferents to the hippocampus of the rabbit. *Journal of Comparative Neurology* **176**, 495–514.

HJORTH-SIMONSEN, A. & ZIMMER, J. (1975) Crossed pathways from the entorhinal area to the fascia dentata. I. Normal in rabbits. *Journal of Comparative Neurology* **161**, 57–70.

HUNTER, A. & STEWART, M. G. (1989) A quantitative analysis of the synaptic development of the lobus parolfactorius of the chick (*Gallus domesticus*). *Experimental Brain Research* **78**, 425–34.

KROUSTRUP, J. P. & GUNDERSEN, H. J. G. (1983) Sampling problems in a heterogeneous organ: A quantitation of relative and total volume of pancreatic islets by light microscopy. *Journal of Microscopy* **132**, 43–55.

LORENTE DE NÓ, R. (1934) Studies on the structure of the cerebral cortex. II. Continuation of the study of the ammonic system. *Journal für Psychologie und Neurologie* **46**, 113–77.

MAYHEW, T. M.& GUNDERSEN, H. J. G. (1996) "If you assume, you can make an ass out of u and me": a decade of the disector for stereological counting of particles in 3D space. *Journal of Anatomy* **188**, 1–15.

MICHEL, R. P. & CRUZ-ORIVE, L. M. (1988) Application of the Cavalieri principle and vertical section method to the lung: estimation of volume and pleural surface area. *Journal of Microscopy*, **150**, 117–36.

NADLER, J. V., PERRY, B. W, GENTRY, C. & COTMAN, C. W. (1980) Loss and reacquisition of hippocampal synapses after selective destruction of CA3-CA4 afferents with kainic acid. *Brain Research* **191**, 387–403.

OORSCHOT, D. E. (1994) Are you using neuronal densities, synaptic densities or neurochemical densities as your definitive data? There is a better way to go. *Progress in Neurobiology* **44**, 233–47.

PAKKENBERG, B. & GUNDERSEN, H. J. G. (1988) Total number of neurons and glial cells in human brain nuclei estimated by the disector and the fractionator. *Journal of Microscopy*, **150**, 1–20.

RICHARDSON, K. C., JARRET, L. & FINKE, E. H. (1960) Embedding in epoxy resins for ultrathin sectioning in electron microscopy. *Stain Technology* **35**, 313–23.

ROYET, J.-P. (1991) Stereology: a method for analyzing images. *Progress in Neurobiology* **37**, 433–474.

SAPER, C. B. (1966) Any way you cut it: a new Journal policy for the use of unbiased counting methods. *Journal of Comparative Neurology* **364**, 5.

SMALL, J. D. (1968) Measurement of section thickness. *Abstracts of the Fourth European Regional Conference on Electron Microscopy (Rome)* **1**, 609–10.

STERIO, D. C. (1984) The unbiased estimation of the number and sizes of arbitrary particles using the disector. *Journal of Microscopy* **134**, 127–36.

SWAAB, D. F. & UYLINGS, H. B. M. (1987) Density measures: parameters to avoid. *Neurobiology of Aging* **8**, 574–6.

WEIBEL, E. R. (1979) *Stereological Methods. Vol. 1. Practical Methods for Biological Morphometry.* New York: Academic Press.

WEST, M. J. (1993) New stereological methods for counting neurons. *Neurobiology of Aging* **14**, 275–85.

WEST, M. J.& GUNDERSEN, H. J. G. (1990) Unbiased stereological estimation of the number of neurons in the human hippocampal formation. *Journal of Comparative Neurology* **296**, 1–22.

WEST, M. J., SLOMIANKA, L. & GUNDERSEN, H. J. G. (1991) Unbiased stereological estimation of the total number of neurons in the subdivisions of the rat hippocampus using the optical fractionator. *Anatomical Record* **231**, 482–97.

WESTRUM, L. E. & BLACKSTAD, T. W. (1962) An electron microscopic study of the stratum radiatum of the rat hippocampus (regio superior, CA1) with particular emphasis on synaptology. *Journal of Comparative Neurology* **119**, 281–309.